Supporting information

Novel thiophene-linked metalloporphyrin conjugated polymer: highly efficient trifunctional electrocatalyst for overall water splitting and oxygen reduction

Song Lu[a]*, Jiadi Ying[a], Tiancun Liu[a], Yeqing Wang[a], Min Guo[a], Qi Shen[a], Qing Li[b]*, Yong Wu[c], Yafei Zhao[d], Zhixin Yu[a]*

[a]Institute of New Energy, School of Chemistry and Chemical Engineering, Shaoxing University, Shaoxing 312000, Zhejiang, China.

[b]Department of Machine Learning, Mohamed bin Zayed University of Artificial Intelligence, Masdar 999041, Abu Dhabi.

[c]School of Chemistry, Dalian University of Technology, Dalian 116024, China.

[d]School of Physics and Engineering, Henan University of Science and Technology, Luoyang 471023, China

Computation details

The binding energy (E_b) of TM atoms embedded into the TP was calculated based on equation S1:

$$E_b = E_{TM-N4/TP} - E_{N4/TP} - E_{TM} \tag{S1}$$

where $E_{TM-N4/TP}$, $E_{N4/TP}$ and E_{TM} are the total energies of TM embedded TP, TM-free TP and TM atoms, respectively.

The cohesive energies of bulk metal materials (E_c) can be calculated by equation S2:

$$E_c = (E_{bulk} - n \times E_{TM})/n \tag{S2}$$

where the E_{bulk} is the energies of bulk metal, E_{TM} is the energies of single metal atoms, and n is the number of metal atom in its bulk structure.

The dissolution ability of TM atoms on support is represented by U_{diss}, which can be calculated by Equation S3 below:
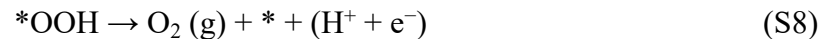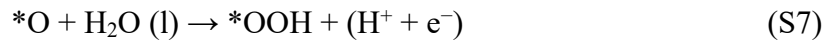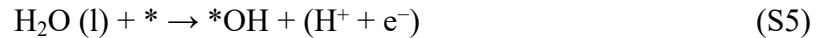
$$U_{diss} = U_0 - (E_b - E_c)/ne \tag{S3}$$

where the U_0 and n denote the standard dissolution potential of TM metal and the number of electron transfer in the dissolution process.

The HER kinetics under equilibrium potential U = 0 and pH = 0 can be expressed by the theoretical exchange current i, according to the equation below:

$$i = -ek \frac{1}{1 + exp(|\Delta G_H|/k_b T)} \tag{S4}$$
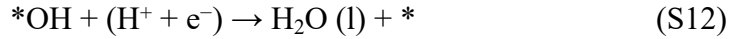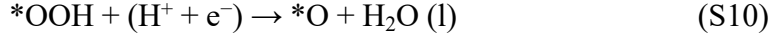
where k is the reaction rate constant, which was set to 1 under η = 0. k_b and T are the Boltzmann constant and temperature, respectively.

The pathways of OER, ORR and HER have been summarized below. Under acidic condition, OER can be divided into the four elementary steps:

$$H_2O\ (l) + * \rightarrow *OH + (H^+ + e^-) \tag{S5}$$

$$*OH \rightarrow *O + (H^+ + e^-) \tag{S6}$$

$$*O + H_2O\ (l) \rightarrow *OOH + (H^+ + e^-) \tag{S7}$$

$$*OOH \rightarrow O_2\ (g) + * + (H^+ + e^-) \tag{S8}$$

where * denotes the catalyst, l and g represent the liquid phase and gas phase. The ORR process can be regarded as the inverse process of the OER process, it can be expressed by steps:

$$O_2\ (g) + * + (H^+ + e^-) \rightarrow *OOH \tag{S9}$$

$$*OOH + (H^+ + e^-) \rightarrow *O + H_2O \text{ (l)} \tag{S10}$$

$$*O + (H^+ + e^-) \rightarrow *OH \tag{S11}$$

$$*OH + (H^+ + e^-) \rightarrow H_2O \text{ (l)} + * \tag{S12}$$

The change of Gibbs free energy for OER steps from ΔG_1 to ΔG_4 can be calculated as below:

$$\Delta G_1 = G(*OH) + G(H^+ + e^-) - G(H_2O) - G(*) \tag{S13}$$

$$\Delta G_2 = G(*O) + G(H^+ + e^-) - G(*OH) \tag{S14}$$

$$\Delta G_3 = G(*OOH) + G(H^+ + e^-) - G(*O) - G(H_2O) \tag{S15}$$

$$\Delta G_4 = G(*) + G(O_2) + G(H^+ + e^-) - G(*OOH) \tag{S16}$$

$$\text{and } G(H^+ + e^-) = G(\frac{1}{2}H_2) \tag{S17}$$

The free energy of O_2 can be obtained by $G(O_{2, }g) + 2G(H_{2, }g) - 2G(H_2O, l) = 4.92$ eV.

The changes of free energy in OER can be described as:

$$\Delta G_1 = G(*OH) \tag{S18}$$

$$\Delta G_2 = G(*O) - G(*OH) \tag{S19}$$

$$\Delta G_3 = G(*OOH) - G(*O) \tag{S20}$$

$$\Delta G_4 = 4.92 - G(*OOH) \tag{S21}$$

Therefore, the free energy changes in ORR processes from ΔG_a to ΔG_d can be expressed as below:

$$\Delta G_a = -\Delta G_4 \tag{S22}$$

$$\Delta G_b = -\Delta G_3 \tag{S23}$$

$$\Delta G_c = -\Delta G_2 \tag{S24}$$

$$\Delta G_d = -\Delta G_1 \tag{S25}$$

The overpotentials of OER and ORR can be calculated by equations below:

$$\eta_{OER} = \max \{\Delta G_1, \Delta G_2, \Delta G_3, \Delta G_4\}/e - 1.23 \tag{S26}$$

$$\eta_{ORR} = \max \{\Delta G_a, \Delta G_b, \Delta G_c, \Delta G_d\}/e + 1.23 \tag{S27}$$

where 1.23 is the equilibrium potential.

Descriptor φ involving the local structural and chemical environment of the reaction site was developed by Xu et al., which can be expressed by equation below:

$$\varphi = \theta_{d} \times \frac{\chi aver}{\chi o}$$

(S28)

where θ_d is the valance electron number of the TM atom, $\chi aver$ denote the average electronegativity of the TM atom and its nearest neighboring N atoms, and χo is the electronegativity of the O atom. $\chi aver$ is calculated as $(\chi TM + n\chi N)/(n + 1)$, where χTM and χN are the electronegativities of the TM and N atoms, respectively, and n is the number of N atoms.

To describe the stability of catalysts under different electrode potentials, we tuned the work function (Φ) of each model to match the applied potential U according to equation below[1]:

$$U/V = (\Phi-4.44)/eV + 0.0592 \text{ pH/V}$$

(S29)

The excess charge was varied from -2.0 e to $+2.0$ e. Where U is the electrode potential, Φ is the work function, 4.44 eV is the work function of the normal hydrogen electrode (NHE), and 0.0592 is the potential change by one pH unit. In this study, we set the pH = 0. We then carried out work function calculations at five different charged states, and extrapolated the electron number e for the Φ at targeted U (Figure S14). Herein, we only consider the Co-N$_4$/TP single atom catalyst as representative for performing calculation under implicit solvent and constant potential due to the big cost of computation resource.

The free energy of the Co ion $G(Co^{2+}(aq))$ is obtained from the experimental standard hydrogen electrode U_0 and the calculated free energy of the bulk metal $G(Co(s))$ as follows[2]:
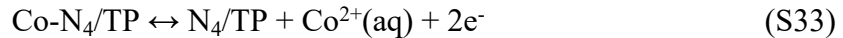
$$Co^{2+}(aq) + 2e^- \leftrightarrow Co\ (s)$$

(S30)

$$G(Co^{2+}(aq)) = G(Co\ (s)) - 2\mu_e$$

(S31)

$$\mu_e = \mu_{SHE} - |e|U_0$$

(S32)

where μ_e denotes the electron energy, μ_{SHE} is benchmarked to be -4.6 eV for VASPsol[3], and $U_0 = -0.28$ V.

The leaching process can be expressed as below:

$$Co-N_4/TP \leftrightarrow N_4/TP + Co^{2+}(aq) + 2e^-$$

(S33)

Therefore, the reaction free energies under a constant potential U can be calculated as

follows:

$$\Delta G = G(N_4/TP*^{Q2}) + G(Co^{2+}(aq)) - G(Cu\text{-}N_4/TP*^{Q1}) + 2|e|U + (Q_2 - Q_1 + 2) \quad (S34)$$

where Q_1 and Q_2 are the net charges on the Cu-N_4/TP and N_4/TP surfaces, respectively. To balance the charge, the number of electrons involved changes to $Q2 + 2 - Q1$.

Table S1. The lattice parameter a with unit Å; The binding energy (E_b) and cohesive energy (E_c) with unit eV; The dissolution potential (U_{diss}) with unit V; the charge transfer with unit e⁻; The Gibbs free energy of *H, *OH, *O, and *OOH with unit eV; the magnetic moment (DFT and DFT+ U) with unit μ_B.

TM-N_4/TP	a	E_b	E_c	U_{diss}	Q_e	ΔG_{*H}	ε_d	ΔG_{*OH}	ΔG_{*O}	ΔG_{*OOH}	Magnetic moment	
											DFT	DFT+U
Sc	14.57	-11.73	-4.21	0.43	1.95	2.35	1.63	-1.10	1.62	2.20	3.00	3.00
Ti	14.50	-11.71	-5.47	1.49	1.70	-0.24	1.32	-1.53	-1.44	2.00	3.89	3.00
V	14.49	-10.83	-5.50	1.49	1.52	0.15	1.85	-1.90	-1.26	0.69	5.31	3.00
Cr	14.55	-9.62	-3.78	2.01	1.38	0.46	2.49	0.31	0.60	3.52	7.99	7.99
Mn	14.42	-9.20	-4.00	1.41	1.49	0.64	0.18	0.93	1.68	4.10	7.00	7.60
Fe	14.45	-9.37	-5.11	1.68	1.24	0.45	-0.084	0.87	1.91	4.07	6.00	6.00
Co	14.47	-9.46	-4.94	1.98	1.01	0.07	-0.48	1.25	2.65	4.12	5.00	4.99
Ni	14.44	-9.35	-5.17	1.83	0.93	1.30	-1.36	2.20	3.90	4.99	4.00	3.99
Cu	14.52	-7.41	-3.85	2.12	1.00	1.98	-2.42	2.41	4.62	5.10	4.50	5.00
Zn	14.58	-6.22	-1.25	1.73	1.20	2.02	-5.7	2.05	4.54	4.86	4.00	4.00
Zr	14.52	-12.13	-6.19	0.04	2.27	-0.97	0.004	-2.56	-1.68	0.80	2.13	2.79
Nb	14.49	-12.57	-8.04	0.41	1.87	-0.64	0.58	-2.10	-5.30	1.30	3.77	4.94
Mo	14.45	-12.41	-8.54	1.09	1.65	-0.33	1.06	-0.77	-1.48	1.38	4.87	4.85
Ru	14.50	-10.73	-7.25	2.20	1.23	-0.5	-0.22	0.25	0.77	3.20	6.00	6.00
Rh	14.51	-10.20	-6.05	2.67	0.91	-0.54	-0.71	0.97	2.57	3.90	5.00	5.00
Pd	14.53	-8.52	-3.70	3.36	0.86	1.52	-2.31	2.53	4.69	5.15	4.00	4.00
Ag	14.61	-5.54	-2.62	3.72	0.87	2.16	-4.02	2.79	5.09	5.43	3.00	5.00
Cd	14.71	-4.83	-0.90	1.57	1.10	1.74	-7.13	1.96	4.39	4.81	4.00	4.00
Hf	14.55	-12.86	-6.45	0.05	2.04	-1.18	0.84	-2.78	-1.68	0.64	3.28	3.60
Ta	14.45	-13.27	-8.74	0.91	2.03	-0.90	-0.09	-2.03	-2.42	-1.84	3.08	3.00
W	14.45	-11.66	-8.38	1.19	1.81	-0.71	0.38	-1.25	-2.19	0.91	4.89	4.64
Re	14.50	-13.77	-10.91	1.25	1.57	-0.64	-0.024	-0.55	-1.54	1.55	7.00	7.00
Os	14.36	-11.33	-8.31	1.22	1.26	-0.80	-0.61	0.15	0.30	2.95	1.82	2.39

Ir	14.47	-11.40	-7.34	2.51	0.93	-0.63	-0.96	1.01	2.24	3.92	4.99	4.99
Pt	14.52	-10.80	-5.53	3.81	0.84	0.96	-2.17	2.48	4.55	5.17	4.00	4.00
Au	14.46	-6.63	-3.08	2.68	0.98	2.26	-5.27	2.82	5.02	5.45	3.00	2.99

Table S2. The atomic number Z; The atomic radius (r) with unit Å; The electronegativity (E_N); The electron affinity (E_A) and the first ionization energy (I_E) with unit eV; The covalent radius (r_{cov}) with unit Å; The oxidation state (σ); the electron number of the d orbital (N_e).

TM-N$_4$/TP	Z	r	E_N	E_A	I_E	r_{cov}	σ	N_e
Sc	21	2.11	1.36	0.19	6.56	1.70	1.95	1.00
Ti	22	1.87	1.54	0.08	6.83	1.60	1.70	2.00
V	23	1.79	1.63	0.53	6.75	1.53	1.52	3.00
Cr	24	1.89	1.66	0.68	6.77	1.39	1.38	5.00
Mn	25	1.97	1.55	-0.50	7.43	1.39	1.49	5.00
Fe	26	1.94	1.83	0.15	7.90	1.32	1.24	6.00
Co	27	1.92	1.88	0.66	7.88	1.26	1.01	7.00
Ni	28	1.63	1.92	1.16	7.64	1.24	0.93	8.00
Cu	29	1.40	1.90	1.24	7.73	1.32	1.00	10.00
Zn	30	1.39	1.65	-0.60	9.39	1.22	1.20	10.00
Zr	40	1.86	1.33	0.43	6.66	1.75	2.27	2.00
Nb	41	2.07	1.59	0.92	6.76	1.64	1.87	4.00
Mo	42	2.09	2.16	0.75	7.09	1.54	1.65	5.00
Ru	44	2.07	2.20	1.05	7.36	1.42	1.23	7.00
Rh	45	1.95	2.28	1.14	7.46	1.42	0.91	8.00
Pd	46	2.02	2.20	0.56	8.34	1.39	0.86	8.00
Ag	47	1.72	1.93	1.30	7.58	1.45	0.87	10.00
Cd	48	1.58	1.69	-0.70	8.99	1.44	1.10	10.00
Hf	72	2.12	1.32	0.18	6.83	1.87	2.04	2.00
Ta	73	2.17	1.51	0.32	7.55	1.70	2.03	3.00
W	74	2.10	2.36	0.82	7.98	1.62	1.81	4.00
Re	75	2.17	1.93	0.06	7.83	1.51	1.57	5.00
Os	76	2.16	2.18	1.08	8.71	1.44	1.26	6.00
Ir	77	2.02	2.20	1.56	8.97	1.41	0.93	7.00
Pt	78	2.09	2.28	2.13	8.96	1.36	0.84	9.00
Au	79	1.66	2.54	2.31	9.23	1.36	0.98	10.00

Figure S1. The total energy and structure variations of metal-free TP at 300 K during AIMD simulation.
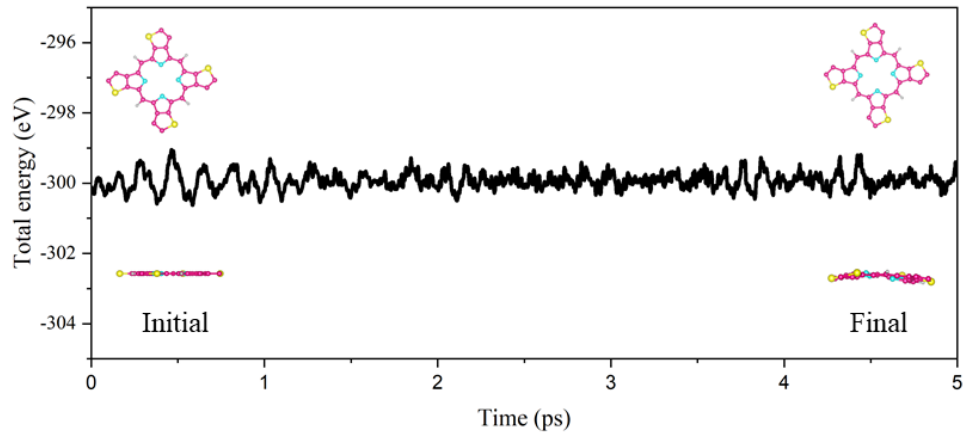

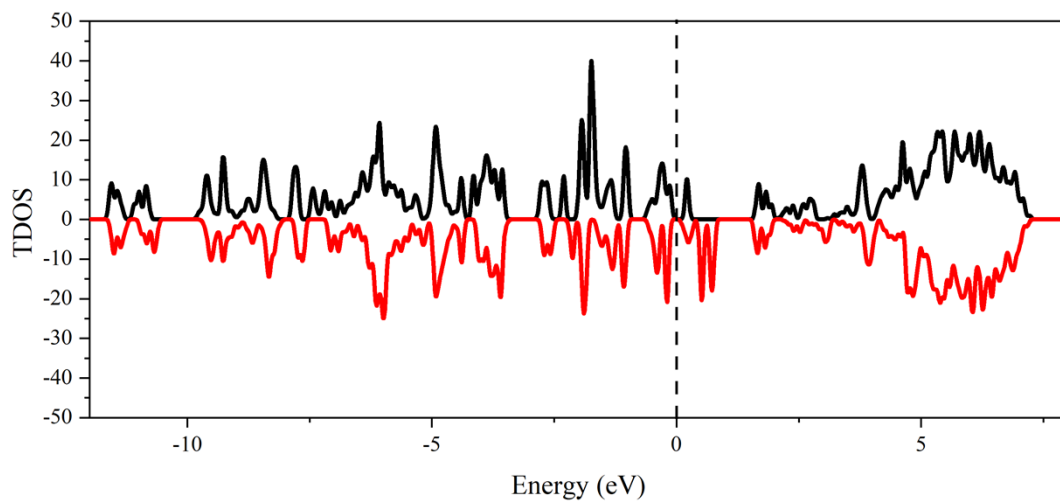Figure S2. The total density of state (TDOS) of metal-free TP.

Figure S3. The calculated phonon dispersion (a) and (b) DOS of Co-N$_4$/TP
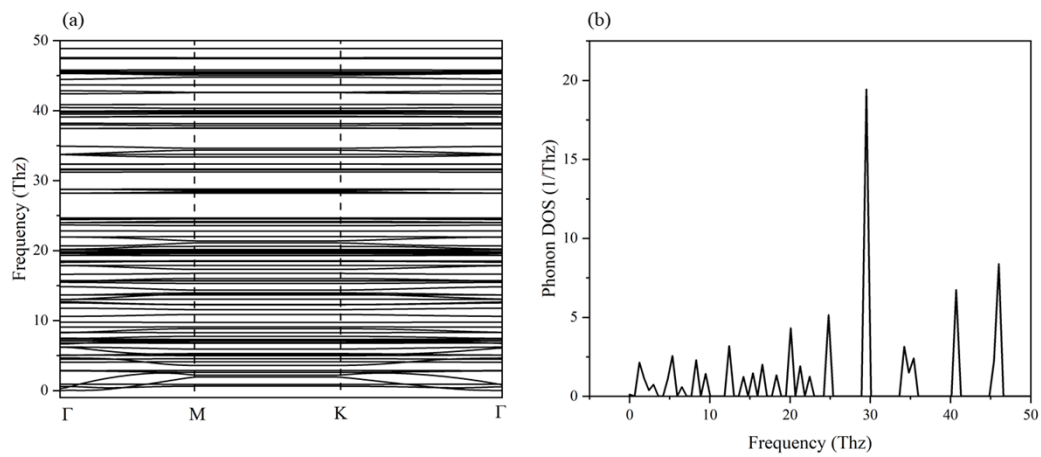

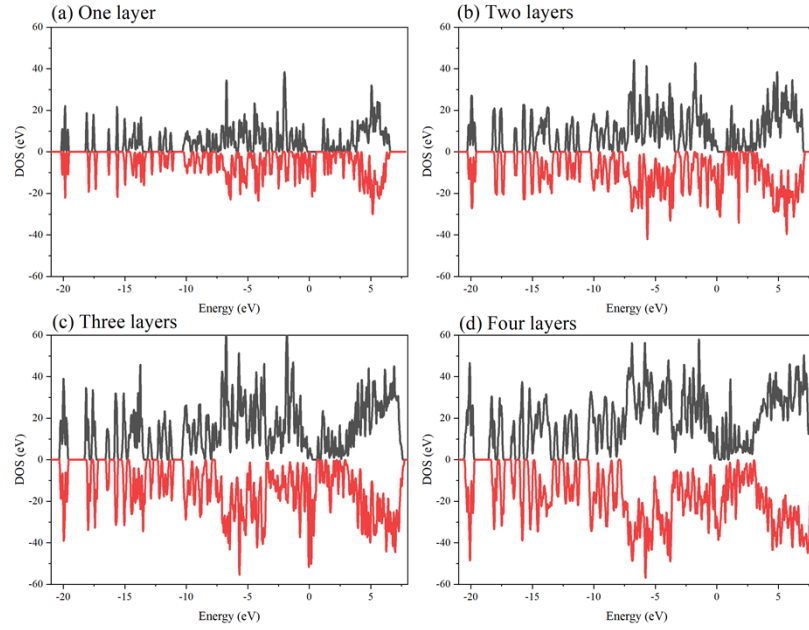Figure S4. The calculated DOS of stacked polymers (a) one layer, (b) two layers, (c) three layers and (d) four layers Co-N$_4$/TP

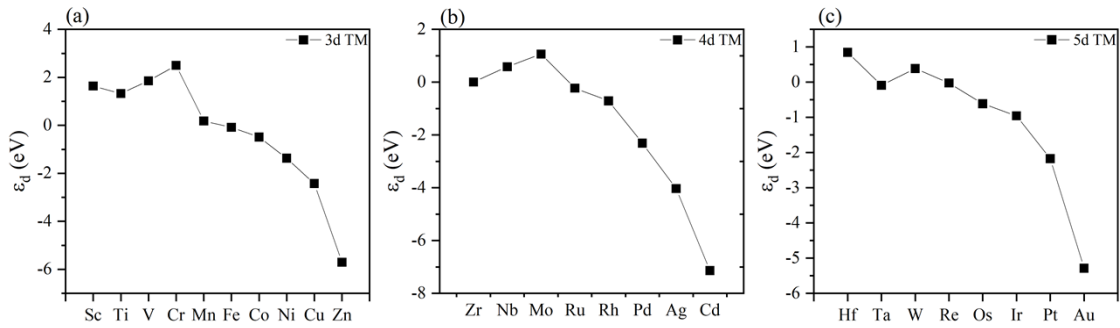Figure S5. The ε_d of (a) 3d TM, (b) 4d TM and (c) 5d TM.

Figure S6. The relationship between ΔG_{*H} and ε_d of (a) 3d TM, (b) 4d TM and (c) 5d TM.
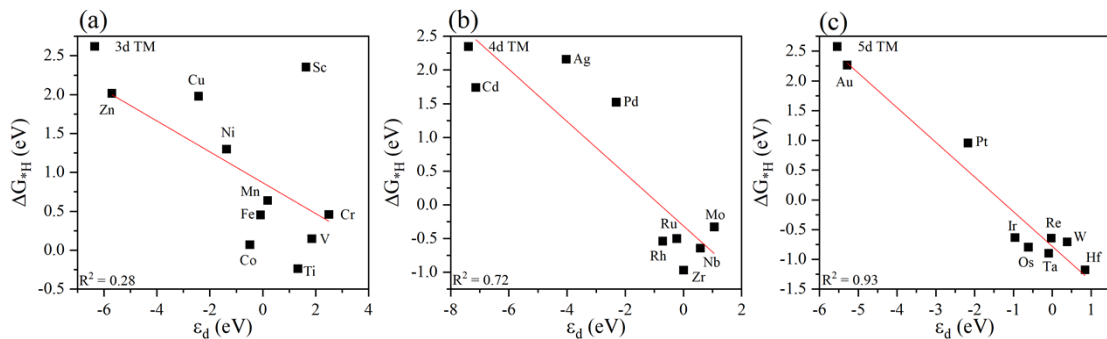
Figure S7. The Gibbs free energy diagrams for the 4e⁻ and 2e⁻ ORR processes of (a) Co-N$_4$/TP, (b) Rh-N$_4$/TP and (c) Ir-N$_4$/TP.
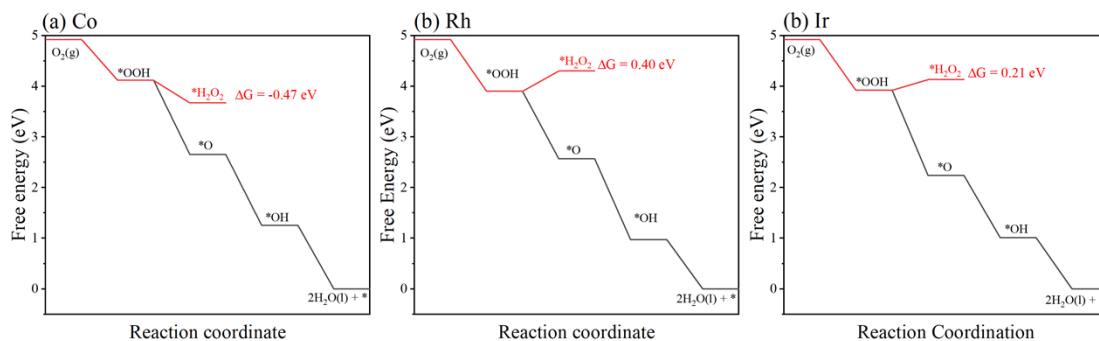
Figure S8. (a) The free energy of Co^{2+}(aq) formation during Co atom leaching at different potentials; (b) The mean square displacement (MSD) of Co atom in three directions; (c) free energy change during the Co atom leaching process under U = −1.5 V (vs. RHE)
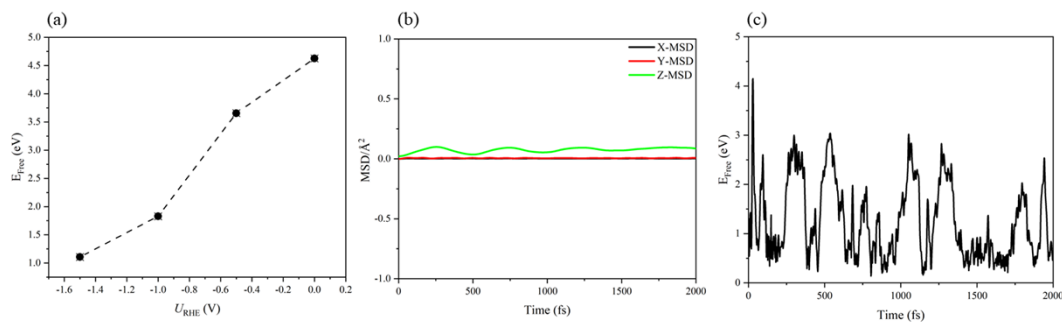
Figure S9. The relationship between (a) ΔG_{*OH} and ε_d, (b) ΔG_{*O} and ε_d, (c) ΔG_{*OOH} and ε_d.
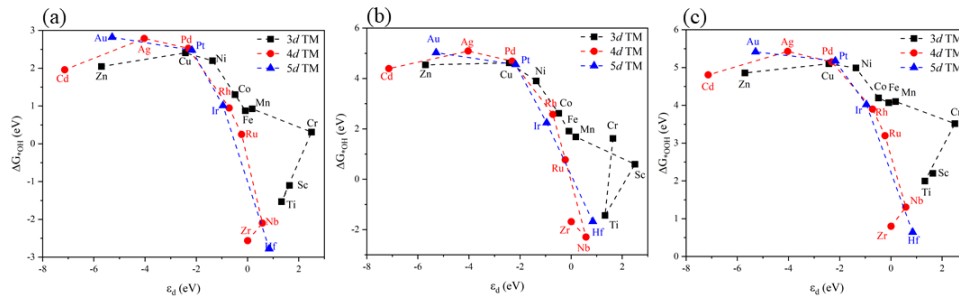
Figure S10. The relationship between (a) ΔG_{*OH} and σ, (b) ΔG_{*O} and (c) ΔG_{*OOH} and σ.
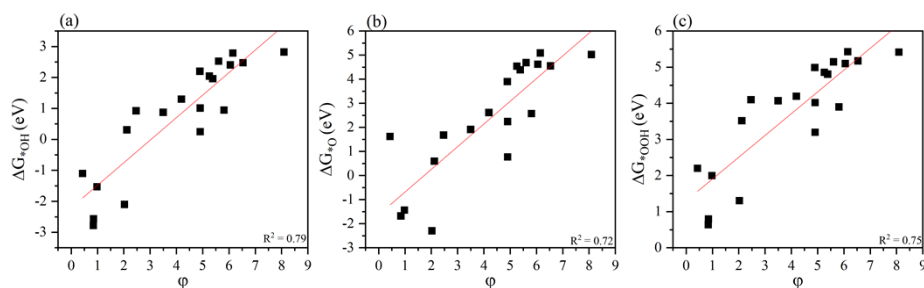

Figure S11. The reversed volcano curves build by (a) the η_{OER} and σ, (b) η_{ORR} and σ.
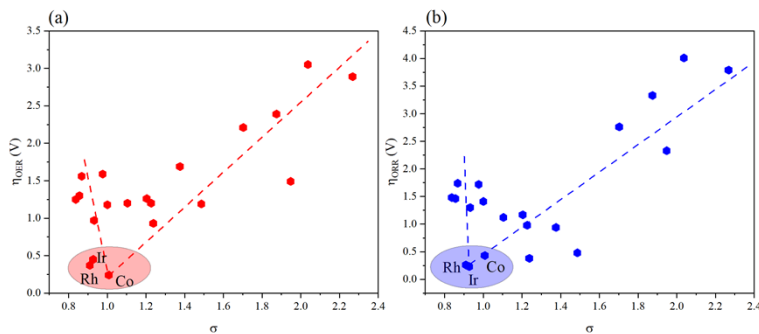

Figure S12.   The COHP of OH adsorption on (a) Co-N_4/TP, (b) Rh-N_4/TP and (c) Ir-N_4/TP.
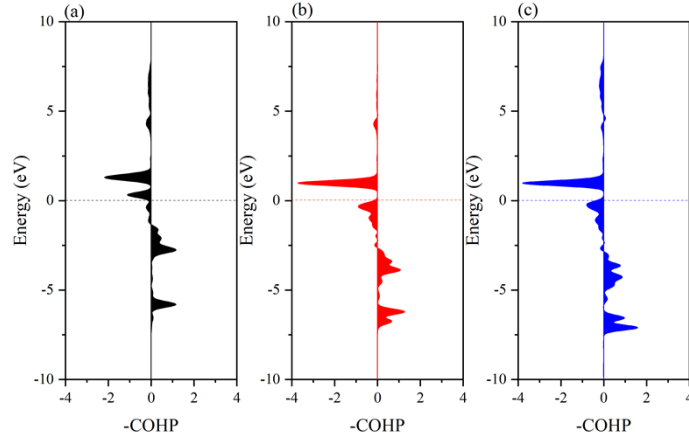
Figure S13. Pearson correlation heatmap for selected descriptors for (a) ΔG_{*H}, (b) ΔG_{*OH}, (c) ΔG_{*O} and (d) ΔG_{*OOH}.
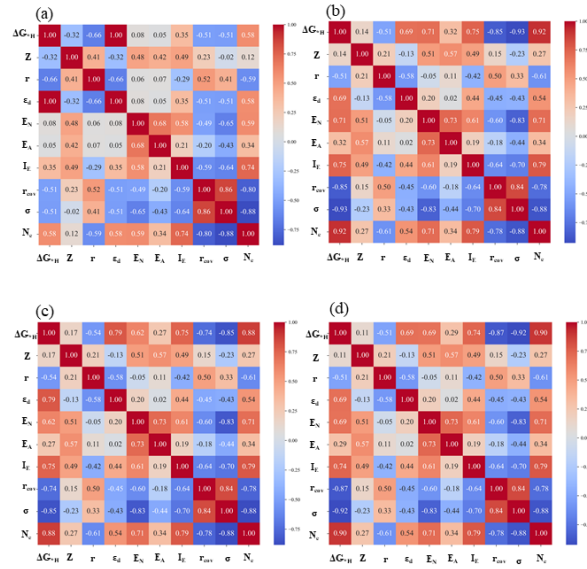

Figure S14. The relationship between work function and charge on (a) Co-N$_4$/TP, (b)N$_4$/TP.

Reference

1. K. Mao, L.J. Yang, X.Z. Wang, Q. Wu, Z. Hu. J. Phys. Chem. Lett. 2020, 11, 8, 2896–2901.

2. X.W. Bai, X.H. Zhao, Y.H. Zhao, Y.H. Zhang, C.Y. Ling, Y.P. Zhou, J.L. Wang. J. Am. Chem. Soc. 2022, 144, 17140−17148

3. K. Mathew, V.S.C. Kolluru, S. Mula, S.N. Steinmann, R.G. Hennig. J. Chem. Phys. 2019, 151, No. 234101.